Modeling rare earth elements binding to humic acids with model VII

Remi Marsac, Charlotte Catrouillet, Mélanie Davranche, Martine Bouhnik-Le Coz, Nicolas Briant, Noémie Janot, Alba Otero-Fariña, Jan E Groenenberg, Mathieu Pédrot, Aline Dia

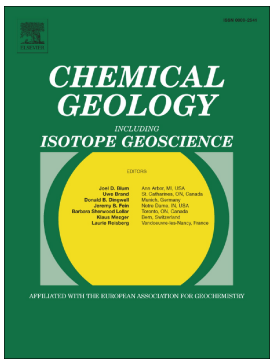

Modeling rare earth elements binding to humic acids with model VII

Rémi Marsac, Charlotte Catrouillet, Mélanie Davranche, Martine Bouhnik-Le Coz, Nicolas Briant, Noémie Janot, Alba Otero-Fariña, Jan E. Groenenberg, Mathieu Pédrot, Aline Dia

PII: S0009-2541(21)00043-7

DOI: https://doi.org/10.1016/j.chemgeo.2021.120099

Reference: CHEMGE 120099

To appear in: *Chemical Geology*

Received date: 25 October 2020

Revised date: 21 January 2021

Accepted date: 27 January 2021

Please cite this article as: R. Marsac, C. Catrouillet, M. Davranche, et al., Modeling rare earth elements binding to humic acids with model VII, *Chemical Geology* (2021), https://doi.org/10.1016/j.chemgeo.2021.120099

Modeling rare earth elements binding to humic acids with Model VII

Rémi Marsac[1,*] remi.marsac@univ-rennes1.fr, Charlotte Catrouillet[1], Mélanie Davranche[1], Martine Bouhnik-Le Coz[1], Nicolas Briant[2], Noémie Janot[3], Alba Otero-Fariña[4], Jan E. Groenenberg[5], Mathieu Pédrot[1], Aline Dia[1]

[1]Univ Rennes, CNRS, Géosciences Rennes - UMR 6118, F-35000 Rennes, France

[2]Laboratoire de Biogéochimie des Contaminants Métalliques, Ifremer, Centre Atlantique, F44311, Nantes Cedex 3, France

[3]ISPA, Bordeaux Sciences Agro, INRAE, F-33140, Villenave d'Ornon, France

[4]School of Earth and Environment, University of Leeds, Leeds LS2 9JT, UK

[5]Soil Chemistry and Chemical Soil Quality, Wageningen University, Wageningen University & Research (WUR), P.O. Box 47, 6700 AA Wageningen, The Netherlands

[*]Corresponding author.

Abstract.

Rare earth elements (REE) naturally occur at trace levels in natural systems but, due to their increasing use in modern technologies, they are now released into the environment, and considered as emerging contaminants. Therefore, the development of numerical predictive models of their speciation in various physico-chemical conditions is required to predict their behavior, transport and potentially toxic effects on ecosystems. Because REE speciation is largely affected by natural organic matter, such as humic acids (HA), this study aimed at calibrating an advanced humic-ion binding model (Model VII) to allow predicting REE-HA binding in various pH conditions, ionic strength and [REE]/[HA], as well as presence of competitor ions. First, REE complexation to monodentate O-containing ligands was evaluated using the Irving-Rossotti equation, which provided constraints for the optimization of REE-HA binding parameters for Model VII. Predictive capacities of Model VII were demonstrated by successfully modeling the effects of various cations (Al^{3+}, Fe^{3+}, Cu^{2+} and Ca^{2+}) and carbonates on REE-HA binding. The large range of physico-chemical conditions for which Model VII is applicable suggest that the present model parameters might be used to more accurately predict the role played by NOM on REE speciation in very contrasting environments, such as in groundwaters, rivers, estuaries, seawater, soils or sediments. Therefore, this study provides a valuable numerical tool to predict the fate of REE in the environment.

I. Introduction

Rare earth elements (REE) are crucial to a wide range of modern technologies. The high demand with respect to global REE production makes them technologically critical elements (TCE). Because of their extensive use, a strong increase of REE release to the environment has been reported worldwide, from rivers, lakes, groundwaters, tap water and coastal seawater (Kulaksız and Bau, 2013 and references therein). Hence, REE are considered as emerging contaminants, whose negative effects on human and environmental health have been suggested (Pagano et al., 2015; 2016; Merschel and Bau, 2015). Since (i) contaminants speciation largely affects their fate in the environment as well as their bioavailability and toxicity, and (ii) REE occurs naturally at trace levels in natural waters (from µg L^{-1} to ng L^{-1} depending on the REE; e.g. Elderfield et al., 1990; Shiolkovitz, 1995; Viers et al., 1997; Dia et al., 2000; Pokrovsky et al., 2005; Tang and Johannesson, 2006; Lerat-Hardy et al., 2019), making REE speciation difficult to measure, it is necessary to develop geochemical speciation models to predict REE speciation in natural systems. Several previous studies showed the high affinity of REE in natural waters for natural organic matter (NOM) such as humic acids (HA) (Dia et al., 2000; Tang and Johannesson, 2003; Sonke and Salters, 2006; Pourret et al., 2007b), so the development of accurate humic-ion binding models for REE is highly required.

One of the most interesting features when studying REE is the high coherence of these elements, whose chemical properties vary regularly along the series, generally divided into three groups: light REE (LREE, La-Nd), middle REE (MREE, Nd-Tb) and heavy REE (HREE, Dy-Lu). This produces "REE patterns" when plotting their relative concentration in an environmental compartment (e.g. water, soil, rock) or a given thermodynamic quantity (e.g. (surface) complexation constants, solubility product) against their atomic number. Their high sensitivity to their coordination environment leads to a large variety of complexation constants patterns depending on the ligand (Byrne and Li, 1995). NOM is a complex mixture of organic compounds bearing various binding functional groups for dissolved cations. In a series of articles, our group demonstrated how the combined effects of NOM site heterogeneity, cation competition and pH could affect REE patterns in natural organic-rich waters (Marsac et al., 2010; 2011; 2012; 2013), where NOM was shown to largely control REE speciation and where other processes (e.g. REE precipitation, sorption to mineral colloids) can be neglected. At circumneutral to slightly alkaline pH, the concentration of major REE competitors for NOM sites (e.g. Al^{3+}, Fe^{3+}) is low due to their low solubility. In such conditions, REE bind to NOM phenolic and chelate ligands, which exhibit larger affinity for HREE than for LREE, hence producing increasing REE patterns for LREE to HREE. At acidic pH, concentrations of competitors for the NOM sites increase (e.g. H^{+}, Al^{3+}, Fe^{3+}). They largely bind to phenolic and chelate ligands, leaving carboxylic as the only available binding sites for REE, which preferentially bind MREE, hence producing convex REE patterns.

REE-HA complexation has been predicted using the humic-ion binding Model VI (Marsac et al., 2011). More recently, a new version of this model was developed (Model VII), whose predictions of humic-ions binding are as accurate as those obtained with Model VI but with smaller number of equations and parameters (Tipping et al., 2011). Furthermore, the Model VII database was extended to account for the binding of many elements in the periodic table, including all REE (Tipping et al., 2011). However, the binding parameters derived by Tipping et al. (2011) shows a continuous increasing series of binding constants for REE binding to humics going from the lightest (La) to the heaviest (Lu). With this parameterization, Model VII might correctly predict REE-HA binding in circumneutral to alkaline conditions with an increasing REE pattern, but it will not be able to predict the convex REE patterns due to preferential binding of the MREE in acidic conditions. There are three possible explanations for this: (i) Tipping et al. (2011) considered a single dataset available in the literature (Sonke and Salters, 2006) to fit REE-HA binding parameters, in which REE-HA patterns only increase from LREE to HREE; (ii) binding parameters for HA carboxylic and phenolic groups cannot be related for REE, because these groups shown distinct REE binding patterns; (iii) the applicability of a linear free energy relationship (LFER), when used for REE, might be limited. The first point is simple to address and the second one has already been pointed out (Marsac et al., 2011). But the latter deserves more attention.

Tipping et al. (2011) applied the approach and findings of Carbonaro and Di Toro (2007) to analyze the Model VII results with LFER. These authors used the equation of Irving and Rossotti (1956) for monodentate ligands with oxygen donor atoms:

$$\log K_{ML} = \alpha_0 \log K_{HL} + \beta_0 \quad (1)$$

where K_{ML} is the metal cation (M)-ligand (L) complexation constant, K_{HL} is the protonation constant of the ligand, α_0 and β_0 are metal cation-dependent parameters. Carbonaro and Di Toro (2007) observed that, for most metal ions investigated, a one-parameter equation (i.e. $\beta_0 = 0$) could be used. Based on this, Tipping et al. (2011) found the following relationship for humic acids to estimate log K_{MA}:

$$\log K_{MA} = 3.51\alpha_0 + 0.74 \quad (2)$$

which relates the logarithm of the average binding constant for carboxylic ligands in Model VII (log K_{MA}) to α_0, the slope of the Irving-Rossotti equation (eq. 1). The existence of such LFER also shows the high consistency of the database for cation-HA binding parameters.

In addition, Carbonaro and Di Toro (2007) investigated only three REE: La, Ce (LREE) and Eu (MREE), omitting the HREE. An evaluation of the whole series, including HREE, is thus required. Finally, the use of equations 1-2 might be limited for REE because Carbonaro and Di Toro (2007)

observed that β_0 values might differ from zero for REE. They discuss this result arguing that both outer-sphere ($K_{ML,os}$, eq. 3), related to β_0 value, and inner-sphere ($K_{ML,is}$, eq. 4) complexes, related to α_0 value, contribute to the overall complexation constant (K_{ML}, as given in eq. 1):

$$M(H_2O)_n^{z+} + L^- \rightleftharpoons (M(H_2O)_n \dots L)^{(z-1)+} \quad ; K_{ML,os} \quad (3)$$

$$(M(H_2O)_n \dots L)^{(z-1)+} \rightleftharpoons (M(H_2O)_{(n-1)}L)^{(z-1)+} + H_2O \quad ; K_{ML,is} \quad (4)$$

The use of the two-parameters Irving-Rossotti equation (eq. 1) for REE revealed an important contribution of outer-sphere complexation, in agreement with Choppin (1997), who determined experimentally that both inner- and outer-sphere complexation occur for Eu binding with haloacetates. Therefore, it might be necessary to account for outer-sphere contribution in REE-ligand complexation to estimate REE-HA binding parameters for Model VII.

This study aims at providing an improved REE-HA parameterization for Model VII, in order to more accurately predict the role played by NOM on REE speciation and REE patterns in various environmental systems. To do so, REE complexation to organic monodentate ligands with oxygen donor atoms will be evaluated using the Irving-Rossotti equation assuming both the formation of inner- and outer-sphere complexes (i.e. $\beta_o \neq 0$). Furthermore, the fitting of Model VII parameters on experimental data will be extended to all existing data sets including the whole REE group. Because both competitive cations and dissolved inorganic ligands can affect REE-HA complexation, the new Model VII parameters will be validated by comparing model results with available experimental data of (i) Fe^{3+}/Al^{3+}-REE competition for HA complexation and (ii) carbonate-HA competition for REE complexation. Additional Cu^{2+}-REE competition experiments will be conducted in order to evaluate the impact of divalent transition metals on REE-HA binding and Model VII predictions.

II. Materials and methods

1. PHREEQC-Model VII

PHREEQC. PHREEQC version 2 (Parkhurst and Appelo, 1999) is a computer code based on an ion-association aqueous model, which was designed to perform speciation and saturation-index calculations in water. The thermodynamic database "Phreeqc.dat" was used. This database has been updated by the incorporation of the well-accepted stability constants at 0 M ionic strength and 25°C for REE inorganic anion complexation relevant to the present work including: (i) chloride ($REECl^{2+}$, $REECl_2^+$) (Luo and Byrne, 2001), (ii) hydroxide ($REEOH^{2+}$, $REE(OH)_2^+$, $REE(OH)_3$) (Klungness and Byrne, 2000), (iii) bicarbonate and carbonate ($REEHCO_3^{2+}$, $REECO_3^+$ and $REE(CO_3)_2^-$) (Luo and Byrne, 2004). Protonation and REE complexation reactions and constants with EDTA

(ethylenediaminetetraacetic acid) were also included (Byrne and Li (1995), and references therein), in order to simulate the experimental conditions of Sonke and Salters (2006).

Model VII. A thorough description of Model VII can be found in Tipping et al. (2011), and its implementation in PHREEQC is described in Marsac et al. (2017). The model is a discrete binding site model which takes electrostatic interactions into account. Only the aqueous cations (e.g. La^{3+}) and their first hydrolysis products (e.g. $LaOH^{2+}$) are considered to bind to HA with the same binding constants. Eight sites are considered and divided into an equal number of type A sites and type B sites, commonly associated with carboxylic and phenolic functional groups, respectively. Proton binding is described by the two median intrinsic protonation constants (pK_A or pK_B) and two parameters defining the spread of the protonation constants around the median (ΔpK_A or ΔpK_B). The intrinsic equilibrium constants for cation binding to type A and type B sites are defined by two parameters ($\log K_{MA}$ and $\log K_{MB}$) and the following equation:

$$\log K_{MB} = \log K_{MA} \times \frac{pK_B}{pK_A} \quad (5)$$

Log K_{MA} is the most important parameter at relatively low pH, whereas log K_{MB} becomes important at higher pH. A fraction of the type A and type B monodentate sites can form bidentate and tridentate sites. The stability constants of these multidentate sites are defined by the sum of the log K values of the monodentate sites of which they are constituted. A small part of the stability constants of multidentate groups are increased by the ΔLK_2 parameter, the so-called "strong binding site term", whose effect is strong at low loadings. The electrostatic correction is represented by an empirical equation that mimics the Boltzmann factor:

$$\exp\left(\frac{-zF\psi}{RT}\right) = \exp(-2PzZI^{0.5}) \quad (6)$$

where P is an adjustable parameter, z is the ion charge, Z is the net humic acid charge (eq g^{-1}), I is the ionic strength (M), ψ is the surface potential (V), T is the temperature (K), F is the Faraday constant and R is the gas constant. This equation cannot be used in PHREEQC but Marsac et al. (2017) showed that it is equivalent to a constant capacitance model (CCM), with a capacitance (C):

$$C = \frac{F^2}{2RTPA_{HA}\log(I)} \quad (7)$$

Given the surface area of HA in Model VII (set as A_{HA} = 1500 m^2 g^{-1}, according to Tipping, 1998), the range of C_1 values found for I < 1 M corresponds to that commonly reported for minerals (0.5 < C_1 < 10 F m^{-2}; Lützenkirchen, 1999).

2. Data selection from the literature

Stability constants for Irving-Rossotti equation analysis. To ensure the consistency between all REE, the stability constants database used in this work includes only studies that report results for the entire REE series (except Pm). REE-monodentate organic ligand stability and acidity constants were taken from Byrne and Li (1995) (and references therein), where all selected constants were obtained at 0.1 M ionic strength and 20°C < T < 25°C. Constants were presently corrected to infinite dilution using the Davies equation. Available organic ligands are formate, acetate, chloroacetate, iodoacetate, propanoate, 3-hydroxopropanoate, benzoate, 3-fluorobenzoate and 4-fluorobenzoate. REE hydrolysis constant at 25°C and 0 M ionic strength were taken from Klungness and Byrne (2000).

REE-HA binding dataset for Model VII parameterization. Only studies reporting results for the entire REE series were selected to determine Model VII parameters. Data were taken from Sonke and Salters (2006), Pourret et al. (2007b) and Marsac et al. (2010). Data of Pourret et al. (2007) and Marsac et al. (2010) refer to multi-REE experiments whereas Sonke and Salters (2006) studied each REE separately and used EDTA as competitive ligand for HA in order to limit REE-HA complexation at high pH and low loadings. Pourret et al. (2007b) investigated the effect of pH on REE-HA binding at relatively high loadings ([HA] = 5, 10, 20 mg L^{-1}; 0.001 M NaCl, 5 µg L^{-1} of each REE). Marsac et al (2010) investigated the effect of [REE]/[HA] at pH = 3 in 0.01 M NaCl. Sonke and Salters (2006) investigated the effect of pH and ionic strength on REE-HA binding at low loading for [HA] = 10 mg L^{-1}, [REE] = 10^{-7} M and [EDTA] = 5×10^{-7} M. The selected dataset covers a large range of pH values (2-9), loadings (10^{-6}-10^{-3} molREE/gHA) and ionic strengths (0.005-0.1 M), which should allow the determination of all Model VII parameters.

REE-HA binding dataset in presence of competitors for Model VII testing. Pourret et al. (2007a) investigated the effect of $NaHCO_3$ (1, 5 and 10 mM) on REE-HA binding for 50 µg L^{-1} of each REE, 5 mg L^{-1} of HA in 10^{-3} M NaCl. In two separate studies, Marsac et al. (2012; 2013) investigated the competitive effect of Al^{3+} and Fe^{3+} on REE-HA binding for Σ[REE] = [Al/Fe] = 10 µM, [HA] = 12 mg L^{-1} and 0.01 M ionic strength (NaCl). Σ[REE] = 10 µM corresponds to 110 µg L^{-1} of each REE, i.e. from 7.9 10^{-7} M to 6.3 10^{-7} M for La and Lu, respectively. Finally, the results of the Ca^{2+}-Eu^{3+} competition experiments conducted by Marang et al. (2008) were also evaluated in the present study, although these data involve a single REE. In the latter study, two series of competitive experiments at pH 5.5 were conducted to evaluate the effect of Eu on Ca binding to HA ([HA] = 200 mg L^{-1}, [Ca] = 30 µM, [KNO_3] = 1 mM, 1 ≤ [Eu] ≤ 50 µM) and the effect of Ca on Eu binding to HA for ([HA] = 15 mg L^{-1}, [Eu] = 5 µM), the latter at different ionic strengths: (i) [KNO_3] = 1 mM for [Ca] < 0.3 mM, (ii) [KNO_3] = 100 mM for 0.3 ≤ [Ca] ≤ 20 mM and (iii) no KNO_3 for [Ca] ≥ 20 mM).

3. REE/Cu-HA binding experiments

Experiments were conducted at Geosciences Rennes in 2011 and, therefore, strictly (i) used the same materials and reagents and (ii) followed the same procedure and (iii) used the same analytical instruments as described in Marsac et al. (2010; 2012; 2013).

All chemicals used were of analytical grade. All experimental solutions were prepared with doubly-deionized water (Milli-Q system, Millipore™). Synthetic REE and Cu solutions were prepared from a nitrate REE and Cu standards (10 mg L^{-1}, Accu Trace™ Reference Standard). Polyethylene containers used to reach complexation equilibrium were all previously soaked in 10% Ultrapure HNO_3 for 48 h at 60°C, then rinsed with deionized water for 24 h at 60°C to remove all REE contamination sources. All experiments were performed at room temperature, i.e. 20°C $\pm$ 2.

Purified humic acid (HA) was obtained from synthetic Aldrich HA (Aldrich™, H1, 675-2). The purification was performed using the Vermeer et al. (1998) protocol, except that a final tangential ultrafiltration step was added to remove any possible HA molecules < 10 kDa using a Labscale TFF system equipped with a Pellicon XL membrane (PLCGC10, Millipore™). Purified HA was freeze-dried and stored in a glass container. Prior to use, it was solubilized overnight in a solution of 0.01 M NaCl at pH = 10 to ensure complete dissolution (Vermeer et al., 1998). The dissolved organic carbon (DOC) concentration was then measured using a Shimadzu 5000 TOC analyzer to assess the exact HA concentration of the experimental suspensions.

The competition effects of Cu on the REE binding by HA were experimentally investigated using a standard batch equilibrium technique. The experimental conditions were: (i) Σ[REE] = [Cu] = 10 µM, (ii) [HA] = 12 mg L^{-1}, and (iii) ionic strength equal to 0.01 M (NaCl). From nitrate standards solutions, the fourteen REE and Cu were simultaneously added to 50 mL HA suspensions. Cu-HA binding experiments in the absence of REE were also conducted at the same Cu concentration (10 µM). REE-HA binding results in the absence of Cu can be found in Marsac et al. (2012). The pH was adjusted from 3 to 6 using 0.1 M HCl/NaOH. During equilibration, solutions were stirred and pH was regularly monitored with a combined Radiometer Red Rod electrode, calibrated with WTW standard solutions (pH 4 and 7). At equilibrium (48 h), 10 mL of the suspension were sampled and ultra-filtered at 5 kDa to separate the metal-HA complexes from the remaining inorganic REE and Cu species. Ultrafiltrations were carried out by centrifuging the solution aliquots through 15 mL centrifugal tubes equipped with permeable membranes of 5 kDa pore size (Vivaspin 15RH12, Sartorius). All the membranes used were first washed with 0.15 M HCl, then rinsed twice with ultrapure water to minimize contamination. Centrifugations were performed using a Jouan G4.12 centrifuge with swinging bucket rotor at 3000g for 30 minutes. All experiments were performed in triplicate. REE and Cu concentrations were determined with an Agilent Technologies™ HP4500 ICP-MS instrument. Ultrafiltrates, containing Cu and REE inorganic species, were directly injected after adding HNO_3 to a concentration of 0.37 N. Quantitative analyses were performed using a conventional external calibration procedure (in 0.37 N HNO_3), which was analyzed every six samples. Three external

standard solutions with REE and Cu concentrations similar to the analyzed samples were prepared from the multi-REE and Cu standard solutions. Indium was added to all samples as internal standard at a concentration of 0.87 μmol L^{-1} to correct for instrumental drift and possible matrix effects. Calibration curves were calculated from the measured REE/indium and Cu/indium intensity ratios. As established from repeated analyses of the multi-REE standard solution and SLRS-4 water standard (Yeghicheyan et al., 2001), the instrumental errors on the REE and Cu analysis are below 3 and 5%, respectively.

III. Results

1. Parameterization of Model VII for REE

1.1. *Evaluation of stability constants for REE-monodentate organic ligands with Irving-Rossotti equation*

Figure 1 plots the stability constants of various REE monodentate O-containing organic ligands complexes (log K_{ML}) against the acidity constant of these ligands (log K_{HL}) for all REE. It also compares the one-parameter ($\alpha_{0\text{-}1}$ with $\beta_0 = 0$ in blue) and the two-parameters ($\alpha_{0\text{-}2}$ with $\beta_0 \neq 0$ in red) linear regressions of the Irving-Rossotti equation (eq. 1), as well as the corresponding coefficients of determination of each REE (R^2; bottom right panel in Figure 1). The one-parameter Irving-Rossotti equation provides a relatively good description of HREE (Tb-Lu) interaction with monodentate ligands ($0.93 < R^2 < 0.96$) but is less appropriate for LREE (La-Gd) ($0.64 < R^2 < 0.85$), which limits inter-REE comparisons (e.g. the study of REE patterns). By contrast, the two-parameters Irving-Rossotti equation provides a better description for all REE ($0.96 < R^2 < 0.99$), as observed by Carbonaro and Di Toro (2007) for La, Ce and Eu, and the similar R^2 values make it suitable for an inter-REE comparison (bottom right panel in Figure 1). Obviously, the log K data are bimodal because of the lack of REE-binding data with relatively strong organic ligands, such as phenols, which affects regression coefficients determination. But, such data are also scarce for many other metal ions (Carbonaro and Di Toro, 2007), so REE are evaluated with a similar approach to other metal ions. Hence, relative REE behavior with respect to that of other metal ions should be consistently captured, which is the major aim of such LFER analysis.

Figure 1. REE complex formation constant (log K_{ML}) with 10 monodentate ligands containing negatively-charged oxygen donor atoms versus the corresponding protonation constant (log K_{HL}) of the ligand (data points). Solid lines represent results from linear regressions using the Irving-Rossotti equation with one-parameter ($\alpha_{0\text{-}1}$ with $\beta_0 = 0$ in blue) and two-parameters ($\alpha_{0\text{-}2}$ and $\beta_0 \neq 0$, in red). Corresponding coefficients of determination (R^2) are shown in the bottom right panel.

Figure 2 shows REE patterns of $\alpha_{0\text{-}2}$ and β_0 fitted with the two-parameters Irving-Rossotti equation. Values of $\alpha_{0\text{-}2}$ increase from La to Lu (Figure 2a), following the reciprocal of REE ionic

radius (Shannon, 1976). In addition, the effect of spin-orbit coupling in 4f electrons on REE-ligand complexation is visible through four "waves" in the pattern, the so-called convex tetrad effect (Kawabe et al., 1999). These observations are consistent with the fact that $\alpha_{0\text{-}2}$ is related to the inner-sphere contribution in REE-ligand complexation (eq. 4; Carbonaro and Di Toro, 2007). The corresponding β_0 values globally decrease along the REE series (Figure 2b). However, this decrease is not linear: β_0 value (i) remains relatively constant between La and Sm, with average at 0.98, (ii) drops between Sm and Tm from 0.97 to 0.43 and (iii) remains constant between Tm and Lu (with average β_0 equal to 0.45). Interestingly, this trend follows the REE coordination number in aquo-complexes, which equals about 9 for LREE (e.g. $La(H_2O)_9^{3+}$) and decreases to about 8 for HREE (e.g. $Lu(H_2O)_8^{3+}$) (Ohta et al., 2008; D'Angelo et al., 2011). Because β_0 is expected to relate to the outer-sphere contribution in REE-ligand complexation, this observation might suggest a relationship between the number of water molecules in the first coordination sphere of the aquo-ion and the formation of outer-sphere complexes in the REE series. Finally, it is worth mentioning that the preferential binding of MREE to monocarboxylic ligands would be mainly due to the large outer-sphere contribution in LREE- and MREE-ligand complexation, according to the evaluation of the Irving-Rossotti equations for REE.

Figure 2a also shows REE patterns of $\alpha_{0\text{-}1}$, obtained from the fitting of the one-parameter Irving-Rossotti equation. Because this single parameter must describe both the inner-sphere and outer-sphere contributions in REE-ligand complexation, $\alpha_{0\text{-}1}$ is a linear combination of $\alpha_{0\text{-}2}$ and β_0:

$$\alpha_{0-1} = \alpha_{0-2} + 0.14\beta_0 \qquad (8)$$

Parameter $\alpha_{0\text{-}1}$ globally increases from La to Lu (like $\alpha_{0\text{-}2}$) but shows a convex shape between La and Gd (inherited from β_0). The impact of the choice of one- or two-parameters equation on the prediction of the REE-ligand stability constants is shown in Figure 2c. REE patterns of log K_{ML} were calculated with both equations for log K_{HL} values equal to 4.1 and 8.3, corresponding to protonation constants of HA carboxylic and phenolic groups in Model VII (pK_A and pK_B), respectively. By using the one-parameter equation, calculated patterns for log K_{HL} = 4.1 and 8.3 show a similar shape. By contrast, the two-parameters equation predicts two distinct patterns for log K_{HL} = 4.1 and 8.3. For log K_{HL} = 8.3, calculated log K_{ML} values only slightly differ between both equations, which leads to similar REE patterns. Therefore, both equations are expected to predict correctly REE complexation patterns with HA phenolic groups (pK_B = 8.3), but only the two-parameters equation can predict REE complexation patterns with HA carboxylic groups (pK_A = 4.1) because it captures REE-ligand pattern variability.

Figure 2. REE patterns of the (a) slope α_0 and (b) y-intercept β_0 of the one- and two-parameters Irving-Rossotti equation. (c) Log K_{ML} patterns for REE calculated for log K_{HL} = 4.1 and 8.3 using the one- and two-parameters equations.

1.2. *Consistency between REE parameters of Irving-Rossotti equation and Model VII*

According to the Irving-Rossotti equation (eq. 1), estimation of log K_{ML} for ligands showing large protonation constants (typically phenolic ligands) will be less affected by the value of β_0 than ligands showing small protonation constants (typically carboxylic ligands). Therefore, log K_{MA} and log K_{MB} can be determined using two different linear combinations of $\alpha_{0\text{-}2}$ and β_0:

$$\log K_{Mi} = U_i \times \alpha_{0-2} + V_i \times \beta_0 + W_i \quad (9)$$

where U_i, V_i and W_i are parameters in eq. 9 that must be determined, with i = A or B. However, because using the one- or two-parameter Irving-Rossotti equations lead to similar REE patterns and stability constant values for log K_{ML} 8.3, log K_{MB} can be estimated by using $\alpha_{0\text{-}1}$ values only. By combining eq. 2 and 5, log K_{MB} was calculated using the same equation as for any metal ion, which should lead to accurate predictions of REE-cation competition for HA phenolic groups:

$$\log K_{MB} = 3.51 \times \frac{pK_B}{pK_A} \times \alpha_{0-1} + 0.74 \times \frac{pK_B}{pK_A} \quad (10)$$

In principle, log K_{MA} for values for the 14 REE could be determined by a fitting U_A, V_A and W_A. However, tests showed that log K_{MA} values determined by Marsac et al. (2011) with the former version of Tipping and coworkers' model (Model VI) could directly be used with Model VII. There are three major reasons for this. First, Model VII is no more than a simplified version of Model VI and both models produce similar results (Tipping et al., 2011). Second, model parameters values for both versions are relatively similar, although larger for Model VII, as shown in Figure 3a by plotting log K_{MA}(Model VII) versus log K_{MA}(Model VI) reported for various cations. Setting log K_{MA} values for REE equal for both models gives consistent results with other cations (see triangles in Figure 3a). Third, U_A, V_A and W_A were determined by a least-square fitting of log K_{MA}(Model VI) values for REE. As shown in Figure 3b, log K_{MA}(Model VI) pattern is relatively well described by the linear combination of $\alpha_{0\text{-}2}$ and β_0 hypothesized in eq. 9:

$$\log K_{MA}\,(Model\ VI) = 1.48 \times \alpha_{0-2} + 0.51 \times \beta_0 + 2.34 \quad (11)$$

This demonstrates that log K_{MA}(Model VI) values determined by Marsac et al. (2011) were already consistent with the presently determined eq. 9. Therefore, in order to limit the number of adjustable parameters, log K_{MA} values in Model VII were set equal to those previously reported for Model VI.

The last parameter of Model VII, ΔLK_2, is not related to Irving-Rossotti equation because it is attributed to either the chelation effect in multidentate ligands or the participation of additional N-, S-

or P-containing functional groups and increases from La to Lu. In order to simplify the parameter fitting procedure, a linear relationship between ΔLK_2(Model VII) and previously determined ΔLK_2(Model VI) (Marsac et al., 2010) was hypothesized and tested:

$$\Delta LK_2(Model\ VII) = V_{\Delta LK2} \times \Delta LK_2(Model\ VI) + W_{\Delta LK2} \quad (12)$$

where $V_{\Delta LK2}$ and $W_{\Delta LK2}$ are parameters that have to be determined. To sum up, only the 2 latter parameters ($V_{\Delta LK2}$ and $W_{\Delta LK2}$ in eq. 12) were adjusted to fit the binding data of the 14 REE to HA, by minimizing the residual sum square on log [REE-HA].

Figure 3. (a) Comparison between Log K_{MA} values for many cations reported in Model VII versus Log K_{MA} values reported in Model VI (data for other cations than REE are from Tipping et al., 2011). (b) Comparison between log K_{MA} values for REE reported for Model VI (Marsac et al., 2011) and calculated with equation 11.

2. Modeling results of REE-HA binding

Figure 4a compares the results of experimental and calculated concentrations of REE bound to HA (plotted as log [REE-HA]) after adjustment of $V_{\Delta LK2}$ and $W_{\Delta LK2}$ parameters (eq. 12) using the data of Sonke and Salters (2006), Pourret et al. (2007b) and Marsac et al. (2010). The average residual equals 0.09 log units. Dotted lines in Figure 4a show that almost all results are predicted within 0.3 log units. The capacity of Model VII to predict accurately REE-HA binding patterns as a function of pH and loading is further illustrated in Figure 4b-f.

Calculations in the experimental conditions of Pourret et al. (2007b) are most affected by log K_{MA} and log K_{MB} values, the effect of ΔLK_2 being minor at high loadings. The effect of pH on REE-HA binding is globally well predicted, although it is overestimated for [HA] = 5 mg L^{-1} (Figure 4b), well predicted for [HA] = 10 mg L^{-1} (Figure 4c) and underestimated and 20 mg L^{-1} (Figure 4d). The increase of HA binding for MREE observed experimentally is well described in simulated patterns, although for lower pH (< 2.5) model predicts a global increase from La to Lu at the largest HA concentration (20 mg L^{-1}).

Calculations in the experimental conditions of Sonke and Salters (2006) are affected by all three Model VII parameters, since the effect of ΔLK_2 becomes important at low loadings. In presence of EDTA, apparent REE-HA complexation constant increases from La to Lu (Sonke and Salters, 2006), but the percentage of REE bound to HA follows the reversed trend due to the competitive effect of EDTA (Figure 4e), which is well predicted by the model, although HREE-HA binding at pH 8.95 is underestimated.

Calculations in the experimental conditions of Marsac et al. (2010) are mostly affected by log K_{MA} and ΔLK_2 values, the effect of log K_{MB} being minor at low pH. Data are presented as distribution

coefficients of REE between HA and the solution (K_d, in L kg_{HA}^{-1}), in order to visualize them all on a single Figure 4f. In these conditions, Model VII results capture well the evolution of REE-HA binding strength and patterns depending on metal loading, with REE-HA binding being weaker (lower K_d values) and patterns showing an increase for MREE at a high loading, whereas REE-HA binding being stronger (lower K_d values) and patterns showing an increase from La to Lu at low loading.

Figure 4. (a) Calculated versus experimental log [REE-HA] for the data of Sonke and Salters (2006), Pourret et al. (2007b) and Marsac et al. (2010). The solid line shows the agreement between model and experiments (1:1 line). Dotted lines show that almost all results are predicted within 0.3 log units. REE-HA pattern of Pourret et al. (2007b), shown as percentage of REE bound to HA, obtained at various pH values for (b) 5, (c) 10 and (d) 20 mg L^{-1} of HA. (e) REE-HA pattern of Sonke and Salters (2006), shown as percentage of REE bound to HA, obtained at various pH and ionic strength (IS) values in presence of EDTA. (f) REE-HA pattern of Marsac et al. (2010), shown as distribution coefficients of REE between HA and the solution (K_d), obtained at various [REE]/[HA] at pH 3. In figure (b)-(f) symbols are experimental data and lines are model results.

IV. Discussion

3. Updated Model VII parameters for REE-HA binding

Model VII parameters obtained in the present work are compared with those determined by Tipping et al. (2011) in Table 1. Because Tipping et al. (2011) only used the data of Sonke and Salters (2006) for Model VII parameterization, presently determined parameter might be more reliable for the prediction of REE-HA complexation on a larger range of physico-chemical conditions, because a larger experimental dataset was used (Sonke and Salters, 2006; Pourret et al., 2007b; Marsac et al., 2010). As stated before, by plotting the values of log K_{MA} of Model VII versus Model VI for all metal ions available, Figure 3a shows that presently determined values might be consistent with other metal ions. Globally, the new log K_{MA} values for REE are larger than the ones determined by Tipping et al. (2011) (except for Tm, Yb and Lu), thus including a stronger binding to carboxylic functional groups, and present log K_{MB} values are smaller than the ones determined by Tipping et al. (2011), thus including a weaker binding to phenolic functional groups. In the present work, the use of eq.10 is expected to ensure that log K_{MB} values for REE are consistent with those of other metal ions in Model VII. Because the data of Sonke and Salters (2006) refer to relatively high pH (≥ 6) and low loading, where log K_{MB} and ΔLK_2 are the most influent parameters, determination of these parameters might be subjected to large uncertainties. As determined previously in Model VI (Marsac et al., 2010), much larger ΔLK_2 values are determined by a fitting procedure than those used by Tipping et al. (2011), estimated using REE-NH_3 complexation constants. In fact, although REE-HA (especially HREE-HA) complexation is strong at low loading, Extended X-ray Absorption Fine Structure analysis showed that the first coordination shell around HREE bond to HA is described by a single HREE–O backscattering path, i.e. the presence of N, S or P was not evidenced (Marsac et al., 2015). As previously observed

(Marsac et al., 2011), the large values of ΔLK_2 for REE might reflect other mechanisms than complexation with N-ligands, such as the chelation effect.

Accurate parameterization of REE-HA, especially REE distribution among the various binding groups in HA, is important to predict REE patterns in the environment. If spectroscopic analysis can determine the average coordination environment of REE bound to HA, they cannot quantify the amount of REE bound to each of the various binding sites. However, cations can affect REE-HA binding by blocking carboxylic, phenolic and/or strong binding sites, which should affect REE-HA patterns depending on their relative affinity for HA binding sites. As in the case of EDTA (Sonke and Salters, 2006), other anions can affect REE-HA patterns because of their preferential binding to LREE, MREE or HREE. They also decrease HA loading by decreasing the amount of REE bound to HA, which is another source or REE-HA pattern variability. Therefore, the reliability of presently determined Model VII parameters, especially their capacity to predict both the amount of REE bound to HA and REE-HA patterns, will be tested by via competitive experiments between (i) REE and other metals for HA binding and (ii) HA and anions for REE binding in the following sections.

Table 1. Comparison of Log K_{MA}, Log K_{MB} and ΔLK_2 determined in the present work and by Tipping et al. (2011). [a] set equal to log K_{MA} values determined for Model VI (Marsac et al., 2010). [b] fixed using eq. 10. [c] fitted to experimental data using eq. 12 as constraint. All the other Model VII parameters were set to the default values provided by Tipping et al. (2011).

	Log K_{MA}		**Log K_{MB}**		**ΔLK_2**	
	Present work[a]	Tipping et al. (2011)	Present work[b]	Tipping et al. (2011)	Present work[c]	Tipping et al. (2011)
La	3.29	2.62	4.92	5.30	2.25	0.11
Ce	3.34	2.66	4.91	5.38	2.28	0.13
Pr	3.36	2.85	4.96	5.77	2.30	0.16
Nd	3.37	2.83	5.06	5.73	2.30	0.18
Sm	3.39	2.93	5.18	5.93	2.35	0.20
Eu	3.36	2.89	5.22	5.85	2.38	0.29
Gd	3.33	2.95	5.08	5.97	2.38	0.24
Tb	3.3	3.04	5.10	6.15	2.45	0.26
Dy	3.27	3.2	5.10	6.48	2.50	0.28
Ho	3.24	3.1	5.12	6.28	2.53	0.30
Er	3.25	3.21	5.10	6.50	2.55	0.32
Tm	3.22	3.23	5.13	6.54	2.65	0.35
Yb	3.19	3.24	5.15	6.56	2.73	0.37
Lu	3.16	3.29	5.15	6.66	2.75	0.39

4. Modeling cation competitive effect on REE-HA binding

Competition with Al(III) or Fe(III). Previous studies investigated the impact of Al(III) or Fe(III) on REE-HA complexation (Marsac et al., 2012; 2013). The authors used 5 kDa filters to separate Al/Fe/REE-HA complexes from dissolved metal ion species. However, the precipitation of

Al/Fe-hydroxides was expected at pH above 4.5, which are also retained by a 5 kDa filter and cannot be distinguished from Al/Fe-HA complexes. Therefore, Figure 5a shows the experimental and predicted percentage of Al/Fe retained by the 5 kDa filters, which is assumed to account for both precipitated and HA-bound Fe and Al species. For both trivalent metals, precipitation was considered via the following reaction:

$$Al/Fe(OH)_{3(s)} + 3H^+ \rightleftharpoons Al/Fe^{3+} + 3H_2O \qquad ; K_S \qquad (13)$$

where solubility products (K_S) equal 10^9 and $10^{5.4}$ for Al and Fe, respectively, which correspond to freshly precipitated (amorphous) solids (Marsac et al., 2012; 2013, and references therein).

For Fe, formation of a polynuclear species was also considered, since spectroscopic studies have shown that HA can stabilize such species of poorly soluble elements, such as Fe(III) (Gustafsson et al., 2007; Karlsson and Persson, 2010; Mikutta and Kretzschmar, 2011; Vantelon et al., 2019), but also Cr(III) (Löv et al., 2017) or Pu(IV) (Marsac et al., 2014). Because these complexes might involve from two to four metal cations, the formation of a trimer was considered for every HA site according to the following reaction:

$$HA^{-n} + 3Fe(OH)_2^+ \rightleftharpoons HA - Fe_3(OH)_6^{(3-n)} \qquad (14)$$

where HA^{-n} is one HA biding site with a charge -n. This reaction is simpler than the corresponding one in Marsac et al. (2013) and comparable to the one used by Marsac et al. (2014) for Pu(IV). Formation constants of HA-Fe(III)-trimer complexes were determined applying the same set of equations as for single metal ions. The value of log K_{MA} for the trimer was determined equal to 6.80 by a fitting procedure, by constraining log K_{MA} value using eq. 5 and setting ΔLK_2(trimer) = 0, Fe(III)-HA binding parameters to the default values (log K_{MA} = 3.37 and ΔLK_2 = 2.20; Tipping et al., 2011) and log K_S = 5.4. The percentage of Fe(III) retained by a 5 kDa filter (i.e. determined by summing the amount of precipitated Fe(III) and Fe(III) bound to HA) versus pH is well predicted in the presence of HA and REE (Figure 5a). Although REE-HA complexation is overestimated by the model at all pH values studied (3-6), as shown for Eu in Figure 5b, the effect of Fe(III) on REE-HA binding patterns is highly consistent with experimental results, as shown at pH 3 (Figure 5c) and 6 (Figure 5d). Thus, at pH 3, Fe(III) competitive effect is slightly stronger for HREE than for LREE (Figure 5c) whereas, at pH 6, Fe(III) competitive effect is similar for all REE (Figure 5d).

For Al, log K_{MA} value had to be slightly increased compared to the one determined by Tipping et al. (2011), from 2.82 to 3.05, to predict the percentage of Al retained by a 5 kDa filter in presence of HA and REE at pH between 3 and 4.5 (Figure 5a). This variation is still smaller than the standard deviation determined on average by Tipping et al. (2011) on log K_{MA} for various cations ($\sigma \approx 0.3$).

This adjustment also improved the prediction of REE-HA complexation (Figures 5b,c) at pH < 4.5. At pH > 4.5, Al-HA complexation cannot solely explain the removal of Al from the solution, but the precipitation of $Al(OH)_{3(s)}$ also plays a role on Al removal. As a consequence, Al-HA complexation is limited. This also limits its competitive effect on REE-HA complexation, which is overestimated by 10-20%, depending on the REE (Figures 5b,d). Aluminum competitive effect on REE might be better predicted by accounting for three different processes. First, other Model VII parameters could be adjusted, a strategy adopted by Marsac et al. (2012). However, it is preferable to keep the number of adjustable parameters as low as possible and a consistent description of humic-ion binding for all cations. Second, the formation of polymeric Al-HA complexes could be included but, to our knowledge, no spectroscopic data provide evidence for such complexes. Third, the adsorption of HA on $Al(OH)_{3(s)}$ might occur, but such modeling exercise is far beyond the scope of this manuscript. Therefore, no attempt was made to improve the simulations in Al-REE system at pH > 4.5. Nevertheless, predicted REE-HA binding patterns remain relatively consistent with experimental ones (Figure 5d).

Figure 5. Comparison of experimental (symbols) and modeling results (lines) for [HA] = 12mg L^{-1}, ∑[REE] = [Al/Fe] = 10 µM in 0.01 M NaCl. (a) Percentage of Al(III) or Fe(III) retained by a 5 kDa filter versus pH in presence of REE. (b) Percentage of Eu-HA complexes in the absence or presence of Al or Fe. REE-HA binding patterns at (c) pH 3 and (d) pH 6 presented as percentage of REE-HA complexes. Error bars on experimental results in percentage, omitted for clarity, are ± 5. Note that different y-axis scales were used for Figure (c) and (d).

Competition with Cu(II). Results of Cu-HA binding are shown in Figure 6a in the absence or the presence of an equal amount of REE at pH between 3 and 6. Log K_{MA} for Cu had to be slightly increased, from 2.38 to 2.55 compared to the generic one determined by Tipping et al. (2011), to predict Cu-HA binding without REE (Figure 6a). This variation is smaller than the standard deviation determined by Tipping et al. (2011) on log K_{MA} for Cu obtained using different datasets (σ = 0.24). The presence of REE decreased drastically Cu-HA binding, which is well predicted by the model (Figure 6a). Conversely, Cu has no significant effect on REE-HA complexation, as show on Figures 6b,c,d. Accordingly, the model predicts almost no Cu competitive effect on REE HA complexation at pH 3 (Figure 6c), and only little effect (5-10% decrease depending on the REE) at pH 6 (Figure 6d). Cu competition is similar for all REE, as observed experimentally and predicted by the model (Figures 6c,d). Therefore, Model VII can accurately predict the effect of Cu on REE-HA binding patterns.

Figure 6. Comparison of experimental (symbols) and modeling results (lines) for [HA] = 12mg L^{-1}, ∑[REE] = [Cu] = 10 µM in 0.01 M NaCl. (a) Percentage of Cu(II)-HA complexes versus pH in the presence (full symbols) or absence of REE (open symbols). (b) Percentage of Eu-HA complexes in the absence or presence of Cu. REE-HA binding patterns at pH 3 (c) and pH (6), presented as percentage of REE-HA complexes. Error bars on experimental results, omitted for clarity, are ± 5. Note that different y-axis scales were used for Figure (c) and (d).

Competition with Ca(II). Although no REE-Ca competition experiments for HA binding are available for the whole REE group, the capacity of Model VII to predict the effect of Ca on Eu-HA complexation was also tested using the experimental data of Marang et al. (2008). Figure 7a shows the percentage of Ca-HA complexes versus total [Eu]. Ca data obtained in the absence of Eu were used to adjust log K_{MA}(Ca) to 1.65 (against 1.30 in Tipping et al., 2011). Predictions made for larger [Eu] gave relatively satisfactory results for Ca-HA binding, although slightly overestimated (as observed in Marang et al., 2008). Predictions of Eu-HA binding (Figure 7a) is also consistent with experimental data, although overestimated at all Ca concentrations. This might be explained by the different HA used in the study of Marang et al. (2008), which requires a slight decrease of log K_{MA}(Eu) to 3.20 (against 3.36 in Table 1) to accurately predict the effect of Ca on Eu binding (dotted line in Figure 7a).

Further simulations were conducted to estimate the effect of Ca on REE-HA patterns, using the same conditions of Marang et al. (2008) but setting equal concentrations of each REE, with ∑[REE] = 5 µM (equal to total [Eu] in the original experiments). Because Ca binds weakly to HA strong sites (ΔLK_2 = 0, Tipping et al., 2011), it has a smaller competitive effect on HREE than on LREE: La-HA and Lu-HA binding decreases down to 21% and 49%, respectively, when [Ca] = 100 mM. This leads to a change in REE-HA pattern, which globally increases from LREE to HREE at high [Ca]. However, the weak binding of Ca to HA cannot suppress REE-HA binding to the weakest carboxylic groups, and REE-HA pattern preserve a convex shape for MREE. These simulations suggest that, if Ca can affect REE-HA binding patterns, the effect is much smaller than that of trivalent elements such as Al^{3+} and Fe^{3+}. Therefore, Ca might only play a role on REE-HA pattern variability in saline conditions (e.g. estuaries or seawaters). This might also be the case for Mg, whose binding parameters for HA are similar to those of Ca (Tipping et al., 2011).

Figure 7. (a) Experimental and modelled (plain line) percentage of Ca-HA complexes versus total [Eu] and Eu-HA complexes versus total [Ca] in the Eu-Ca competition experiments of Marang et al. (2008) (see "Data selection from the literature" section for experimental conditions details). Dotted lines correspond to model calculation with slightly adjusted value of log K_{MA}(Eu). (b) Predicted REE-HA binding patterns in the experimental conditions of Marang et al. (2008), but setting equal concentrations of each REE, with ∑[REE] = 5 µM.

5. Modeling the effect of carbonates on REE-HA binding

The effect of carbonates on REE-HA complexation has been investigated by Pourret et al. (2007a). Experiments and modeling results with Model VII are shown in Figure 8. The percentage of REE bound to HA decreases with increasing [$NaHCO_3$] and increasing pH, because CO_3^{2-} is a stronger aqueous ligand than HCO_3^- for REE. The effect of carbonates on REE-HA complexation is weak for LREE (e.g. La, Figure 8a), intermediate for MREE (e.g. Eu, Figure 8b) and strong for HREE (e.g. Lu, Figure 8c) because REE-carbonate complexation constants increase from La to Lu (Luo and Byrne, 2004). Model VII predicts relatively well LREE-HA binding at any pH and [$NaHCO_3$] (Figure 8a).

MREE-HA binding is well predicted for pH < 9.5, but the model overestimates it for pH > 9.5 (Figure 8b). This overestimation for pH > 9.5 is even more pronounced for HREE (Figure 8b) than for MREE, and depends on [$NaHCO_3$]. This might be explained by the database used for aqueous complexes because it only takes into account the formation of REE-HCO_3^{2+}, REE-CO_3^{+} and REE-$(CO_3)_2^{-}$ species (Luo and Byrne, 2004), whereas formation of tri- and tetra-carbonato complexes have been evidenced for REE and their trivalent actinide analogues (Am, Cm) in aqueous solutions (Janicki and Lindqvist-Reis, 2018). Although such discrepancies at high pH will have little impact on the prediction of REE speciation in most of environmental systems whose pH globally range from 4 to 9, the impact of tricarbonato complex on Eu-HA binding was tested by using the formation constant of $Am(CO_3)_3^{3-}$ (Guillaumont et al., 2003). Results are shown as dotted lines on Figure 8b, validating the hypothesis that the formation of $Eu(CO_3)_3^{3-}$ might, indeed, explain the discrepancies between experiments and modeling for pH > 9.5. Further experimental studies are required to predict REE speciation in conditions of alkaline pH and high carbonate concentrations.

By contrast with LREE and MREE, HREE-HA binding is slightly underestimated at pH < 9.5. This might be due to the formation of ternary REE-carbonate-HA complexes (Kouhail et al., 2019). Although the authors made this observation for a single MREE (Eu), formation of HREE-carbonate-HA complexes might be more pronounced due to their stronger binding to both HA and CO_3^{2-} than LREE and MREE. Because of the limited dataset available for the whole REE group, and the relatively small discrepancies between experimental and model results (i.e. maximum 15% for Lu; see Figure 8c), no attempt to include ternary REE-carbonate-HA complexes in Model VII was made. As illustrated on Figure 8d for [$NaHCO_3$] = 5 mM and pH < 9.5, REE-HA binding patterns decrease from La to Lu, which is relatively well predicted by Model VII. Note that the anomalous behavior of Yb compared to Tm and Lu is an artifact of the calculation, arising from either a slightly inaccurate Model VII parameter or Yb-carbonate complexation constant.

Figure 8. Observed (symbols) and predicted (lines) effect of carbonates on REE-HA complexation. Percentage of (a) La-HA, (b) Eu-HA (c) and Lu-HA complexes versus pH and [$NaHCO_3$]. Dotted lines correspond to simulations that include the formation of tricarbonato complex for Eu (not available for all REE). (d) REE-HA binding patterns versus pH for [$NaHCO_3$] = 5 mM (only data at pH < 9.5 are shown). Error bars on experimental results, omitted for clarity, are ± 5.

V. Conclusions

Rare earth elements complexation to monodentate O-containing ligands was evaluated using the Irving-Rossotti equation, which relates the affinity of a ligand for the proton to its affinity for a metal ion. In agreement with the preliminary work of Carbonaro and Di Toro (2007), in which only three REE were studied, linear equations involving an intercept provided the best prediction of REE-monodentate ligands binding, confirming that both inner- and outer-sphere complexation contribute to REE-monodentate ligand complexation (Choppin, 1997; Carbonaro and Di Toro, 2007). Derived

REE-HA binding parameters for the humic-ion binding Model VII agreed with parameters of the Irving-Rossotti equation. The model could accurately predict REE-HA binding over a large range of pH values, ionic strengths and [REE]/[HA] conditions.

Predictive capacities of the model were further tested by comparing model calculations to experimental results of cations or ligands competition experiments. Model VII could predict the effect Al(III) and Fe(III) on REE-HA binding. With protons, these metal ions are major competitors for REE, which are expected to largely control REE-HA binding patterns in natural surface waters (Marsac et al., 2013). New experiments were conducted with Cu^{2+}, chosen as a representative divalent transition metal. Only little effect of Cu on REE-HA binding was observed in our experimental conditions ($\sum$[REE] = [Cu]), in agreement with model predictions. However, if Cu^{2+} alone might not affect significantly REE-HA binding patterns, other divalent transition metals occur in natural waters, soils and sediments. This is especially the case under reducing conditions such as in flooded wetlands soils, where reductive dissolution of Fe(III) (hydr)oxides release high amounts of Fe^{2+} to the solution, which can bind to HA (Catrouillet et al., 2014), that might affect REE-HA binding. The presently determined REE-HA binding parameter might help predicting the combined competitive effects of divalent transition metals with either Fe^{3+} in oxidizing conditions or Fe^{2+} in reduced environments. Although it was only tested for a single REE (Eu) in the present study, Model VII predicts relatively small effect of Ca on REE-HA pattern in freshwaters, suggesting that Ca exerts only a small control of REE patterns variability when REE speciation is dominated by NOM. Because Model VII was previously shown to model accurately the effect of high ionic strengths (Marsac et al., 2017), REE patterns could also be predicted in highly saline waters. Finally, Model VII can also predict REE-HA binding patterns in the presence of ligands such as carbonates, although further work is required in order to account for the formation of (i) ternary carbonate-REE-HA complexes for the whole REE group and (ii) tri- and tetra-carbonato complexes with all REE, in order to predict REE speciation under very alkaline conditions (pH > 9).

The successful prediction of REE-HA binding under various pH, ionic strength and [REE]/[HA], as well as in presence of various cations (Al^{3+}, Fe^{3+}, Cu^{2+} and Ca^{2+}) and carbonates suggest that Model VII can be used to more accurately predict the role played by NOM on REE speciation in very contrasted environments (e.g. fresh waters, seawater, soils or sediments). Because Model VII is already used to evaluate the toxicity of some metal ions towards aquatic organisms (Stockdale et al., 2010), the present study might also help determining REE bioavailability and toxicity in future studies. In addition to speciation calculations, PHREEQC can also perform reactive transport modeling. Therefore, PHREEQC-Model VII coupling might also be used to predict the transport of REE in the environment. However, if the present study provides a valuable predictive tool of REE speciation and REE patterns in organic-rich waters, the impact of NOM quality requires further work. For instance, NOM of bacterial origin might produce different REE binding patterns than the humic fractions presently evaluated (Catrouillet et al., 2019). In environmental systems

characterized by high physico-chemical gradients and under the influence of various biogeochemical factors, such as flooded soils (Davranche et al., 2011) or estuaries (Dulaquais et al., 2018), large spatial and temporal variability in NOM composition occurs. Finally, NOM fractionation at mineral-water interface might also contribute to NOM variability in natural systems (Janot et al., 2012; Reiller, 2012; Janot et al., 2013) and might affect REE speciation. Therefore, further work is required in order to account for the variability in NOM composition and reactivity towards REE.

The following are the supplementary data related to this article.

Supplementary information: A PHREEQC database necessary to simulate REE and proton binding to HA with Model VII is provided in Appendix. Users should refer to Marsac et al. (2017) for appropriate use of PHREEQC-Model VII, especially to generate input files. A table containing new REE-Cu-HA data is provided in Appendix.

Acknowledgments

This work was supported by the C-FACTOR project funded by ANR (project number ANR-18-CE01-0008). Through the support of the GeOHeLiS analytical platform of Rennes 1 University, this publication is also supported by the European Union through the European Regional Development Fund (FEDER), the French ministry of Higher Education and Research, the French Region of Brittany and Rennes Metropole.

Declaration of interests

The authors declare that they have no known competing financial interests or personal relationships that could have appeared to influence the work reported in this paper.

The authors declare the following financial interests/personal relationships which may be considered as potential competing interests:

References

Byrne R. H. and Li B. (1995) Comparative complexation behavior of the rare earths. *Geochimica et Cosmochimica Acta* **59**, 4575–4589.

Carbonaro R. F. and Di Toro D. M. (2007) Linear free energy relationships for metal-ligand complexation: Monodentate binding to negatively-charged oxygen donor atoms. *Geochimica et Cosmochimica Acta* **71**, 3958–3968.

Catrouillet C., Davranche M., Dia A., Bouhnik-Le Coz M., Marsac R., Pourret O. and Gruau G. (2014) Geochemical modeling of Fe(II) binding to humic and fulvic acids. *Chemical Geology* **372**, 109–118.

Catrouillet C., Guenet H., Pierson-Wickmann A.-C., Dia A., LeCoz M. B., Deville S., Lenne Q., Suko Y. and Davranche M. (2019) Rare earth elements as tracers of active colloidal organic matter composition. *Environ. Chem.* **17**, 133–139.

Choppin G. R. (1997) Inner versus outer sphere complexation of f-elements. *Journal of Alloys and Compounds* **249**, 9–13.

D'Angelo P., Zitolo A., Migliorati V., Chillemi G., Duvail M., Vitorge P., Abadie S. and Spezia R. (2011) Revised ionic radii of lanthanoid(III) ions in aqueous solution. *Inorg. Chem.* **50**, 4572–4579.

Davranche M., Grybos M., Gruau G., Pédrot M., Dia A. and Marsac R. (2011) Rare earth element patterns: a tool for identifying trace metal sources during wetland soil reduction. *Chemical Geology* **284**, 127–137.

Dia A., Gruau G., Olivié-Lauquet G., Riou C., Molénat J. and Curmi P. (2000) The distribution of rare earth elements in groundwaters: assessing the role of source-rock composition, redox changes and colloidal particles. *Geochimica et Cosmochimica Acta* **64**, 4131–4151.

Dulaquais G., Breitenstein J., Waeles M., Marsac R. and Riso R. (2018) Measuring dissolved organic matter in estuarine and marine waters: size-exclusion chromatography with various detection methods. *Environ. Chem.* **15**, 436–449.

Elderfield H., Upstill-Goddard R. and Sholkovitz E. R. (1990) The rare earth elements in rivers, estuaries, and coastal seas and their significance to the composition of ocean waters. *Geochimica et Cosmochimica Acta* **54**, 971–991.

Guillaumont R., Fanghänel T., Fuger J., Grenthe I., Neck V., Palmer D. A. and Rand M. H. (2003) Update on the chemical thermodynamics of uranium, neptunium, plutonium, americium and technetium. *Chemical Thermodynamics* **5**.

Gustafsson J. P., Persson I., Kleja D. B. and Van Schaik J. W. J. (2007) Binding of iron(III) to organic soils: EXAFS spectroscopy and chemical equilibrium modeling. *Environmental Science and Technology* **41**, 1232–1237.

Irving H. and Rossotti H. (1956) Some relationships among the stabilities of metal complexes. *Acta Chem. Scand.* **10**, 72–93.

Janicki R. and Lindqvist-Reis P. (2018) Eu(III) and Cm(III) tetracarbonates – in the quest for the limiting species in solution. *Dalton Trans.* **47**, 2393–2405.

Janot N., Reiller P. E. and Benedetti M. F. (2013) Modelling Eu(III) speciation in a Eu(III)/PAHA/α-Al_2O_3 ternary system. *Colloids and Surfaces A: Physicochemical and Engineering Aspects* **435**, 9–15.

Janot N., Reiller P. E., Zheng X., Croué J.-P. and Benedetti M. F. (2012) Characterization of humic acid reactivity modifications due to adsorption onto α-Al_2O_3. *Water Research* **46**, 731–740.

Karlsson T. and Persson P. (2010) Coordination chemistry and hydrolysis of Fe(III) in a peat humic acid studied by X-ray absorption spectroscopy. *Geochimica et Cosmochimica Acta* **74**, 30–40.

Kawabe I., Ohta A., Ishii S., Tokumura M. and Miyauchi K. (1999) REE partitioning between Fe-Mn oxyhydroxide precipitates and weakly acid NaCl solutions: Convex tetrad effect and fractionation of Y and Sc from heavy lanthanides. *Geochem. J.* **33**, 167–179.

Klungness G. D. and Byrne R. H. (2000) Comparative hydrolysis behavior of the rare earths and yttrium: the influence of temperature and ionic strength. *Polyhedron* **19**, 99–107.

Kouhail Y. Z., Benedetti M. F. and Reiller P. E. (2019) Formation of mixed Eu(III)-CO3-fulvic acid complex: Spectroscopic evidence and NICA-Donnan modeling. *Chemical Geology* **522**, 175–185.

Kulaksız S. and Bau M. (2013) Anthropogenic dissolved and colloid/nanoparticle-bound samarium, lanthanum and gadolinium in the Rhine River and the impending destruction of the natural rare earth element distribution in rivers. *Earth and Planetary Science Letters* **362**, 43–50.

Lerat-Hardy A., Coynel A., Dutruch L., Pereto C., Bossy C., Gil-Diaz T., Capdeville M.-J., Blanc G. and Schäfer J. (2019) Rare Earth Element fluxes over 15 years into a major European Estuary (Garonne-Gironde, SW France): Hospital effluents as a source of increasing gadolinium anomalies. *Science of The Total Environment* **656**, 409–420.

Löv Å., Sjöstedt C., Larsbo M., Persson I., Gustafsson J. P., Cornelis G. and Kleja D. B. (2017) Solubility and transport of Cr(III) in a historically contaminated soil – Evidence of a rapidly reacting dimeric Cr(III) organic matter complex. *Chemosphere* **189**, 709–716.

Luo Y.-R. and Byrne R. H. (2004) Carbonate complexation of yttrium and the rare earth elements in natural waters. *Geochimica et Cosmochimica Acta* **68**, 691–699.

Luo Y.-R. and Byrne R. H. (2001) Yttrium and rare earth element complexation by chloride ions at 25°C. *Journal of Solution Chemistry* **30**, 837–845.

Lützenkirchen J. (1999) The constant capacitance model and variable ionic strength: An evaluation of possible applications and applicability. *Journal of Colloid and Interface Science* **217**, 8–18.

Marang L., Reiller P. E., Eidner S., Kumke M. U. and Benedetti M. F. (2008) Combining spectroscopic and potentiometrie approaches to characterize competitive binding to humic substances. *Environmental Science and Technology* **42**, 5094–5098.

Marsac R., Banik N. L., Lützenkirchen J., Catrouillet C., Marquardt C. M. and Johannesson K. H. (2017) Modeling metal ion-humic substances complexation in highly saline conditions. *Applied Geochemistry* **79**, 52–64.

Marsac R., Banik N. L., Marquardt C. M. and Kratz J. V. (2014) Stabilization of polynuclear plutonium(IV) species by humic acid. *Geochimica et Cosmochimica Acta* **131**, 290–300.

Marsac R., Davranche M., Gruau G., Bouhnik Le Coz M. and Dia A. (2011) An improved description of the interactions between rare earth elements and humic acids by modeling: PHREEQC-Model VI coupling. *Geochimica et Cosmochimica Acta* **75**, 5625–5637.

Marsac R., Davranche M., Gruau G. and Dia A. (2010) Metal loading effect on rare earth element binding to humic acid: Experimental and modelling evidence. *Geochimica et Cosmochimica Acta* **74**, 1749–1761.

Marsac R., Davranche M., Gruau G., Dia A. and Bouhnik-Le Coz M. (2012) Aluminium competitive effect on rare earth elements binding to humic acid. *Geochimica et Cosmochimica Acta* **89**, 1–9.

Marsac R., Davranche M., Gruau G., Dia A., Pédrot M., Le Coz-Bouhnik M. and Briant N. (2013) Effects of Fe competition on REE binding to humic acid: Origin of REE pattern variability in organic waters. *Chemical Geology* **342**, 119–127.

Marsac R., Davranche M., Morin G., Takahashi Y., Gruau G., Briant N. and Dia A. (2015) Effect of loading on the nature of the REE–humate complexes as determined by Yb^{3+} and Sm^{3+} L_{III}-edge EXAFS analysis. *Chemical Geology* **396**, 218–227.

Merschel G. and Bau M. (2015) Rare earth elements in the aragonitic shell of freshwater mussel *Corbicula fluminea* and the bioavailability of anthropogenic lanthanum, samarium and gadolinium in river water. *Science of The Total Environment* **533**, 91–101.

Mikutta C. and Kretzschmar R. (2011) Spectroscopic Evidence for Ternary Complex Formation between Arsenate and Ferric Iron Complexes of Humic Substances. *Environ. Sci. Technol.* **45**, 9550–9557.

Ohta A., Kagi H., Tsuno H., Nomura M. and Kawabe I. (2008) Influence of multi-electron excitation on EXAFS spectroscopy of trivalent rare-earth ions and elucidation of change in hydration number through the series. *American Mineralogist* **93**, 1384–1392.

Pagano G., Guida M., Siciliano A., Oral R., Koçbaş F., Palumbo A., Castellano I., Migliaccio O., Thomas P. J. and Trifuoggi M. (2016) Comparative toxicities of selected rare earth elements: Sea urchin embryogenesis and fertilization damage with redox and cytogenetic effects. *Environmental Research* **147**, 453–460.

Pagano G., Guida M., Tommasi F. and Oral R. (2015) Health effects and toxicity mechanisms of rare earth elements—Knowledge gaps and research prospects. *Ecotoxicology and Environmental Safety* **115**, 40–48.

Parkhurst D. L. and Appelo C. A. J. (1999) User's guide to PHREEQC (Version 2): a computer program for speciation, batch-reaction, one-dimensional transport, and inverse geochemical calculations, Water-resources Investigation Report 99–4259. USGS, Denver, Colorado.

Pokrovsky O. S., Dupré B. and Schott J. (2005) Fe–Al–organic Colloids Control of Trace Elements in Peat Soil Solutions: Results of Ultrafiltration and Dialysis. *Aquat Geochem* **11**, 241–278.

Pourret O., Davranche M., Gruau G. and Dia A. (2007a) Competition between humic acid and carbonates for rare earth elements complexation. *Journal of Colloid and Interface Science* **305**, 25–31.

Pourret O., Davranche M., Gruau G. and Dia A. (2007b) Rare earth elements complexation with humic acid. *Chemical Geology* **243**, 128–141.

Reiller P. E. (2012) Modelling metal–humic substances–surface systems: reasons for success, failure and possible routes for peace of mind. *Mineralogical Magazine* **76**, 2643–2658.

Shannon R. D. (1976) Revised effective ionic radii and systematic studies of interatomic distances in halides and chalcogenides. *Acta Cryst, A* **32**, 751–767.

Sholkovitz E. R. (1995) The aquatic chemistry of rare earth elements in rivers and estuaries. *Aquatic Geochemistry* **1**, 1–34.

Sonke J. E. and Salters V. J. M. (2006) Lanthanide–humic substances complexation. I. Experimental evidence for a lanthanide contraction effect. *Geochimica et Cosmochimica Acta* **70**, 1495–1506.

Stockdale A., Tipping E., Lofts S., Ormerod S. J., Clements W. H. and Blust R. (2010) Toxicity of proton–metal mixtures in the field: Linking stream macroinvertebrate species diversity to chemical speciation and bioavailability. *Aquatic Toxicology* **100**, 112–119.

Tang J. and Johannesson K. H. (2006) Controls on the geochemistry of rare earth elements along a groundwater flow path in the Carrizo Sand aquifer, Texas, USA. *Chemical Geology* **225**, 156–171.

Tang J. and Johannesson K. H. (2003) Speciation of rare earth elements in natural terrestrial waters: assessing the role of dissolved organic matter from the modeling approach. *Geochimica et Cosmochimica Acta* **67**, 2321–2339.

Tipping E. (1998) Humic Ion-Binding Model VI: An Improved Description of the Interactions of Protons and Metal Ions with Humic Substances. *Aquatic Geochemistry* **4**, 3–47.

Tipping E., Lofts S. and Sonke J. E. (2011) Humic Ion-Binding Model VII: a revised parameterisation of cation-binding by humic substances. *Environ. Chem.* **8**, 225–235.

Vantelon D., Davranche M., Marsac R., Fontaine C. L., Guénet H., Jestin J., Campaore G., Beauvois A. and Briois V. (2019) Iron speciation in iron–organic matter nanoaggregates: a kinetic approach coupling Quick-EXAFS and MCR-ALS chemometrics. *Environ. Sci.: Nano* **6**, 2641–2651.

Vermeer A. W. P., Van Riemsdijk W. H. and Koopal L. K. (1998) Adsorption of humic acid to mineral particles. 1. Specific and electrostatic interactions. *Langmuir* **14**, 2810–2815.

Viers J., Dupré B., Polvé M., Schott J., Dandurand J.-L. and Braun J.-J. (1997) Chemical weathering in the drainage basin of a tropical watershed (Nsimi-Zoetele site, Cameroon) : comparison between organic-poor and organic-rich waters. *Chemical Geology* **140**, 181–206.

Yeghicheyan D., Carignan J., Valladon M., Bouhnik-Le Coz M., Cornec F. L., Castrec-Rouelle M., Robert M., Aquilina L., Aubry E., Churlaud C., Dia A., Deberdt S., Dupré B., Freydier R., Gruau G., Hénin O., Kersabiec A.-M. de, Macé J., Marin L., Morin N., Petitjean P. and Serrat

E. (2001) A Compilation of Silicon and Thirty One Trace Elements Measured in the Natural River Water Reference Material SLRS-4 (NRC-CNRC). *Geostandards Newsletter* **25**, 465–474.